ORTA DOĞU TEKNİK ÜNİVERSİTESİ
MIDDLE EAST TECHNICAL UNIVERSITY

NATO SET -277 Panel

Inter-Panel / Inter-Group Workshop on
"Phenomenology and Exploitation of Hyperspectral Sensing within NATO"

Target Rediscovery on Long-wave Infrared Hyperspectral Images using Radiance and Emissivity Data

Alper Koz[1], İlke Belenoğlu[2], Mustafa Kütük[1], Esen Yüksel[2], A. Aydın Alatan[1]

[1] Center for Image Analysis, Middle East Technical University, Ankara, 06800, Turkey

[2] Electrical and Electronics Engineering, Hacettepe University, 06800, Ankara

13-14 October 2019
Royal Military Academy,
Brussels, Belgium

OUTLINE

- Problem Description and Existing Works
- Proposed Target Detection Methodologies for LWIR and SWIR hyperspectral images
- Results with respect to different algorithms for SWIR hyperspectral images
- Results for LWIR hyperspectral images
  - Comparison of pixel, group of pixel, and superpixel based detection
  - Comparison with respect to radiance data and emissivity data
  - Comparison with respect to LWIR and SWIR spectrum
- Conclusions

TARGET REDISCOVERY PROBLEM

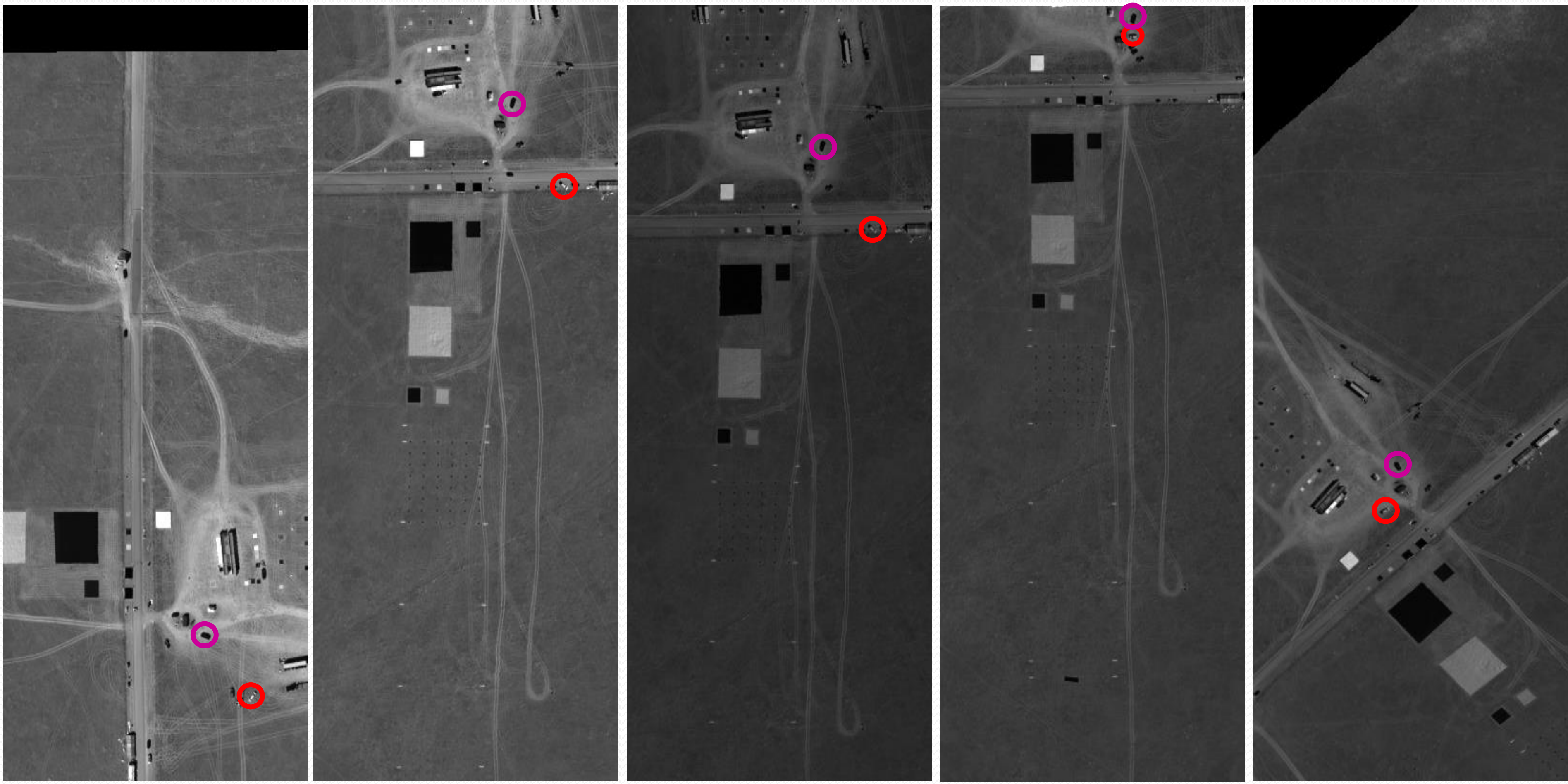

SN3515_20140812T171045_0001 SN3515_20140812T173230_0002 SN3515_20140812T173812_0002 SN3515_20140812T171547_0002 SN3515_20140812T172543_0002

- Find the target in subsequent images of the same scene

PREVIOUS WORK ON TARGET REDISCOVERY

- A few work by Kerekes et al [1] and Uzkent et al. [2] to perform detection and tracking by selecting and weighting certain wavelengths in VNIR range.
- No work on target rediscovery on LWIR hyperspectral images to the knowledge of the authors
- Recent studies on target identification on LWIR hyperspectral images by Rankin et al. [3] and Wurst et al. [4]

Proposed Target Detection Methodologies Target Detection on LWIR Images

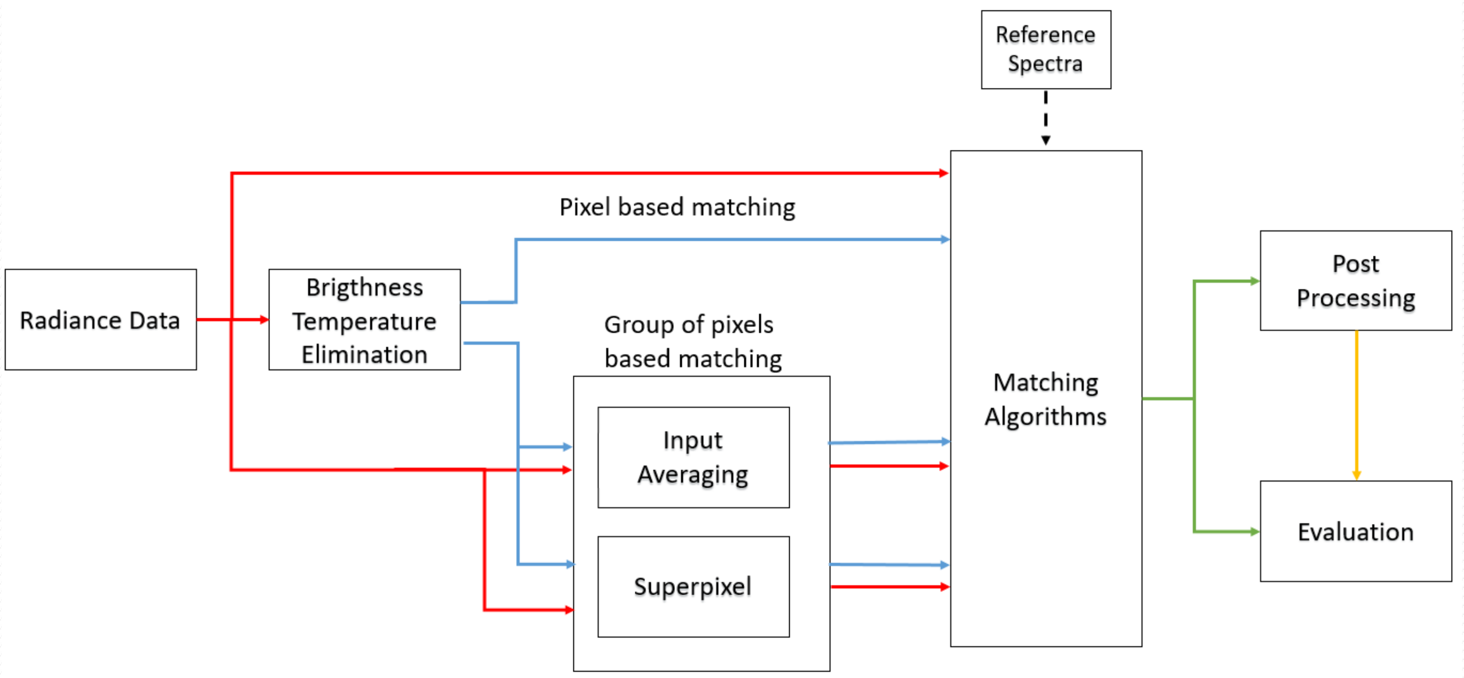

Reference Spectra:

- Target Radiance/Emissivity obtained from previously captured hyperspectral image
- Emissivity signatures measured at ground

Proposed Target Detection Methodologies Brightness Temperature Elimination (1)

Algorithm for Brighness-Temperature Estimation:

- For each pixel of the hyperspectral image, the radiance change of the pixel is assigned to a vector.
- Beginning from a minimum temperature, Tmin, to a maximum temperature, Tmax, Planck curves [11] are generated for the thermal range of LWIR camera with a step size of temperature, ΔT.
- The brightness-temperature corresponding to the generated curve, which is closest to the radiance change of the pixel in MSE sense, is assigned as the brightness-temperature of that pixel.
- The Planck curve generated for the estimated brightness-temperature is substracted from the radiance spectra and inputted to the target detection algorithm.

Proposed Target Detection Methodologies Brightness Temperature Elimination (2)

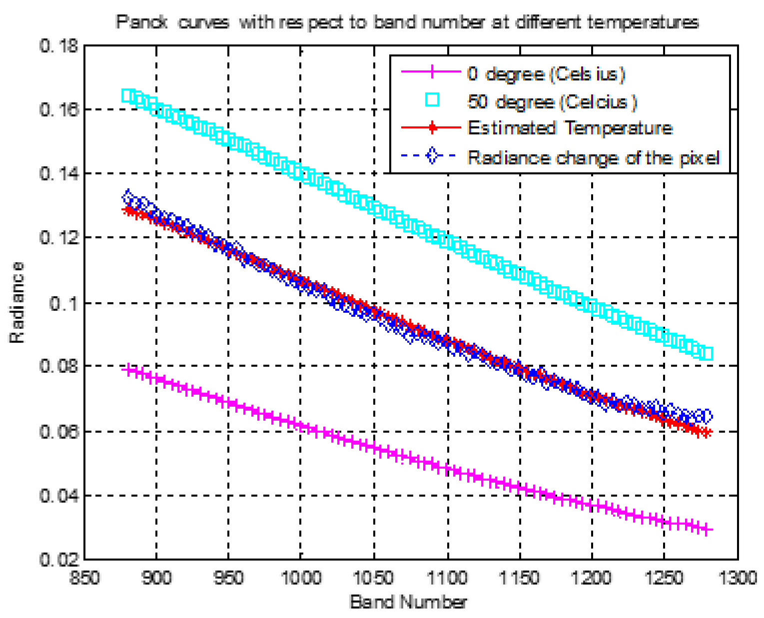

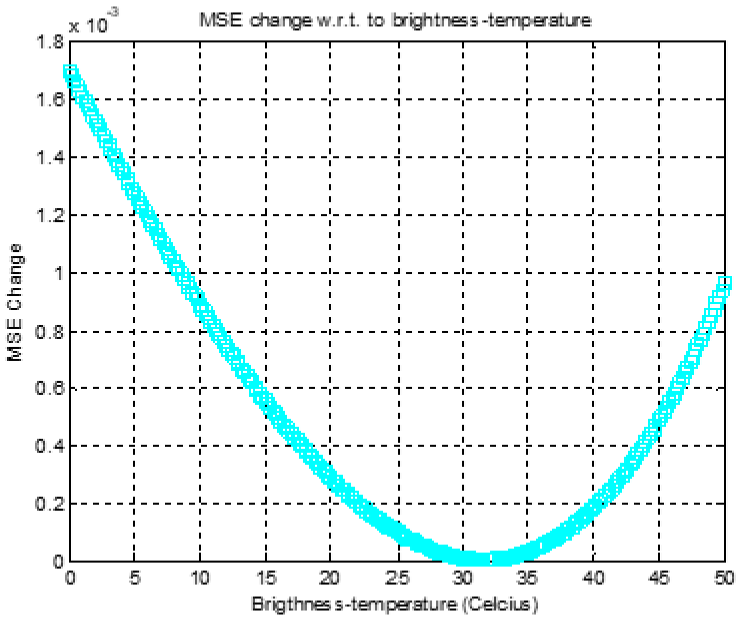

- Take the difference of the radiance spectra (blue) and Planck Curve for the estimated britghness temperature (red).
- This difference can be regarded as an *approximation of emissivity* or *detailed component* of the radiance spectra involving the characteristical information about the pixel.
- Input the difference as a signature to the target detection algorithms.

Proposed Target Detection Methodologies
Utilized Filters for Group of Pixels

```
filt = [ 3 3 3
         3 4 3
         3 3 3];
```

(Weighted averaging)

```
filt = [-1 -1 -1 -1 -1 -1 -1;
        -1 -1 -1 -1 -1 -1 -1;
        -1 -1  3  3  3 -1 -1;
        -1 -1  3  4  3 -1 -1;
        -1 -1  3  3  3 -1 -1;
        -1 -1 -1 -1 -1 -1 -1;
        -1 -1 -1 -1 -1 -1 -1];
```

(Difference of averages)

Proposed Target Detection Methodologies Oversegmentation and Superpixels

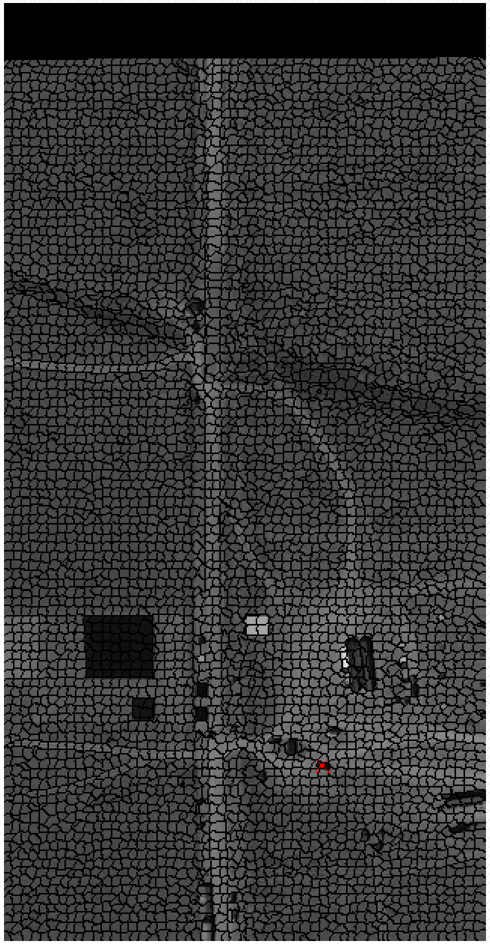

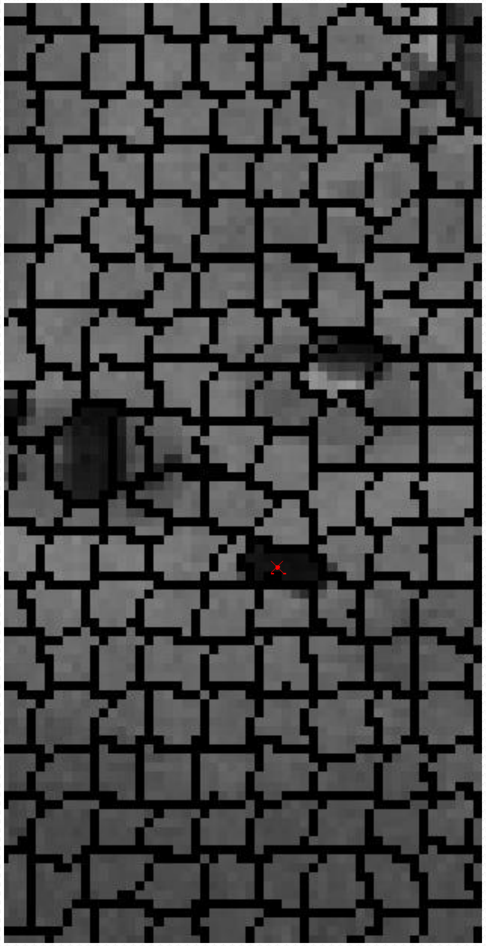

Proposed Target Detection Methodologies
Utilized Algorithms

Representatives from 4 class of target detection methods:

- SAM
  - $H_0: \boldsymbol{x} = \boldsymbol{b} \sim N(0, \boldsymbol{\sigma}^2 I)$
  - $H_1: \boldsymbol{x} = \alpha\boldsymbol{s} + \boldsymbol{b} \sim N(\alpha s, \boldsymbol{\sigma}^2 I)$
  - $T_{SAM}(\boldsymbol{x}) = arccos\left(\frac{\boldsymbol{s}^T\boldsymbol{x}}{(\boldsymbol{s}^T\boldsymbol{x})^{\frac{1}{2}}(\boldsymbol{x}^T\boldsymbol{x})^{\frac{1}{2}}}\right)$

Proposed Target Detection Methodologies
Utilized Algorithms

Representatives from 4 class of target detection methods:

- ACE
  - $H_0: \boldsymbol{x} = \boldsymbol{b} \sim N(0, \boldsymbol{\sigma}_0^2 \Sigma)$
  - $H_1: \boldsymbol{x} = \alpha \boldsymbol{s} + \beta \boldsymbol{b} \sim N(\alpha \boldsymbol{s}, \boldsymbol{\sigma}_1^2 \Sigma)$
  - $T_{ACE}(\boldsymbol{x}) = \dfrac{\boldsymbol{x}^T \Sigma^{-1} \boldsymbol{s} (\boldsymbol{s}^T \Sigma^{-1} \boldsymbol{s})^{-1} \boldsymbol{s}^T \Sigma^{-1} \boldsymbol{x}}{\boldsymbol{x}^T \Sigma^{-1} \boldsymbol{x}}$

Proposed Target Detection Methodologies
Utilized Algorithms

Representatives from 4 class of target detection methods:

- OSP
  - $H_0: \boldsymbol{x} = \alpha_{b,0}\boldsymbol{b} + \boldsymbol{n} \sim N\left(\alpha_{b,0}\boldsymbol{b}, \boldsymbol{\sigma}_0^2\boldsymbol{I}\right)$
  - $H_1: \boldsymbol{x} = \alpha\boldsymbol{e} + \boldsymbol{n} = \alpha_s\boldsymbol{s} + \alpha_{b,0}\boldsymbol{b} + \boldsymbol{n} \sim N\left(\alpha_s\boldsymbol{s} + \alpha_{b,0}\boldsymbol{b}, \boldsymbol{\sigma}_1^2\boldsymbol{I}\right)$
  - $T_{OSP}(\boldsymbol{x}) = \dfrac{\boldsymbol{s}^T(\boldsymbol{b}(\boldsymbol{b}^T\boldsymbol{b})^{-1}\boldsymbol{b}^T)\boldsymbol{x}}{\boldsymbol{s}^T(\boldsymbol{b}(\boldsymbol{b}^T\boldsymbol{b})^{-1}\boldsymbol{b}^T)\boldsymbol{s}}$

Proposed Target Detection Methodologies
Utilized Algorithms

Representatives from 4 class of target detection methods:

- HSD
  - $H_0: \boldsymbol{x} = \alpha_{b,0}\boldsymbol{b} + n \sim N(\alpha_{b,0}\boldsymbol{b}, \boldsymbol{\sigma}_0^2\Sigma)$
  - $H_1: \boldsymbol{x} = \alpha\boldsymbol{e} + \boldsymbol{n} = \alpha_s\boldsymbol{s} + \alpha_{b,1} + n \sim N(\alpha_s\boldsymbol{s} + \alpha_{b,1}\boldsymbol{b}, \boldsymbol{\sigma}_1^2\Sigma)$
  - $T_{HSD}(\boldsymbol{x}) = \frac{(\boldsymbol{x}-\widehat{\alpha}_b\boldsymbol{b})^T\Sigma^{-1}(\boldsymbol{x}-\widehat{\alpha}_b\boldsymbol{b})}{(\boldsymbol{x}-\widehat{\alpha}\boldsymbol{e})^T\Sigma^{-1}(\boldsymbol{x}-\widehat{\alpha}\boldsymbol{e})}$

Proposed Target Detection Methodologies
Target Detection on SWIR Images

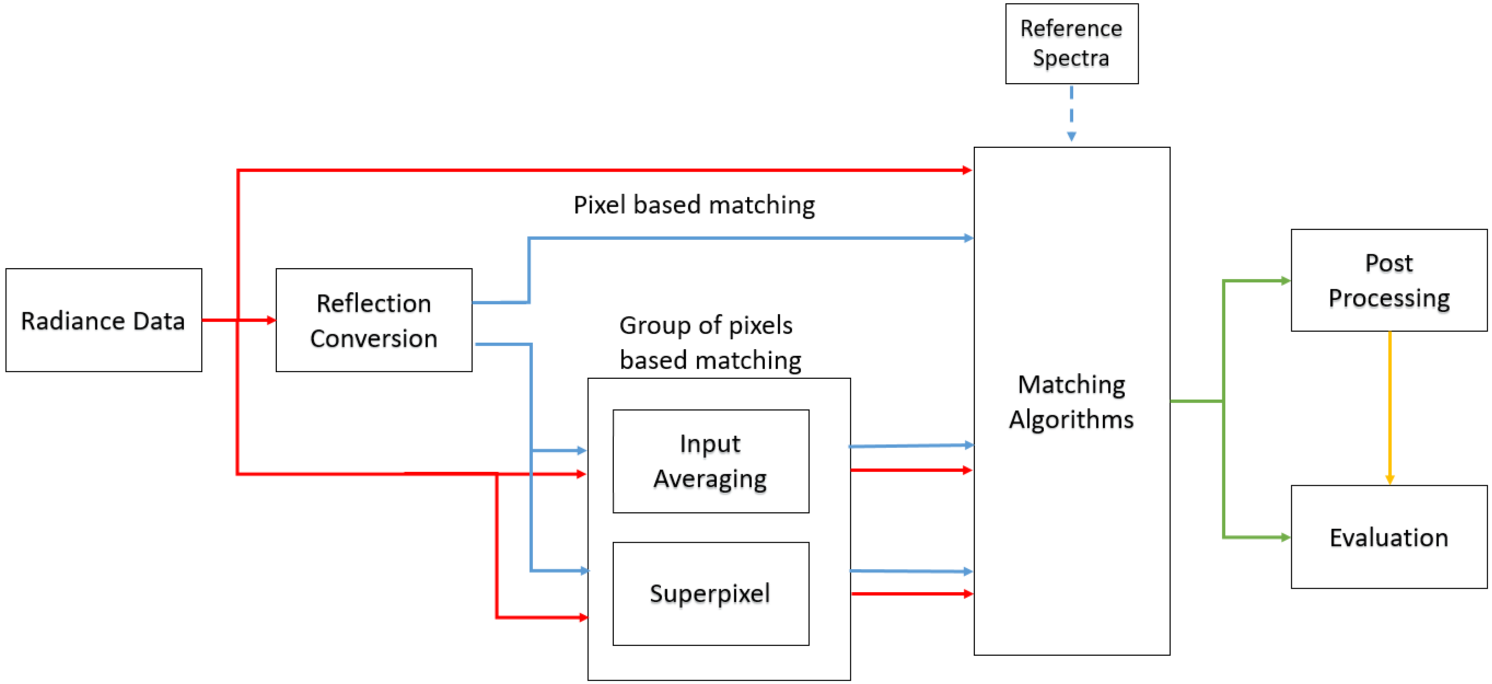

Reference Spectra:

- Target Radiance/Reflectance from previously captured hyperspectral image
- Reflectance signatures measured at ground

Selected SWIR Images and Ground Truths Set 1 (NEO_Hyspex)

SN3515_20140812T171045_0001

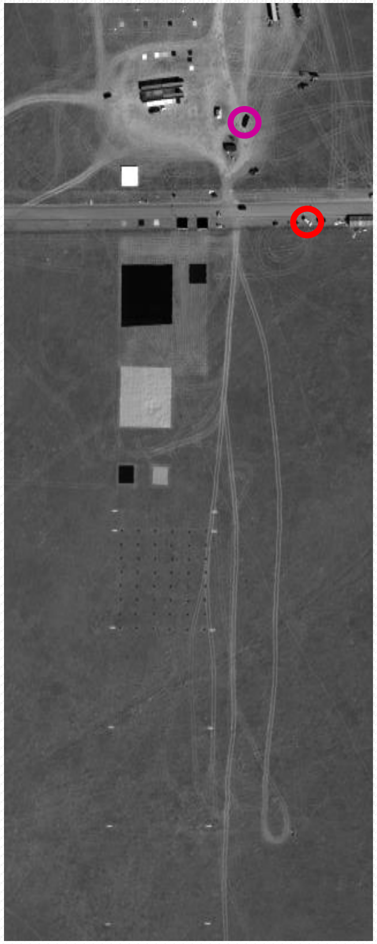

SN3515_20140812T173230_0002

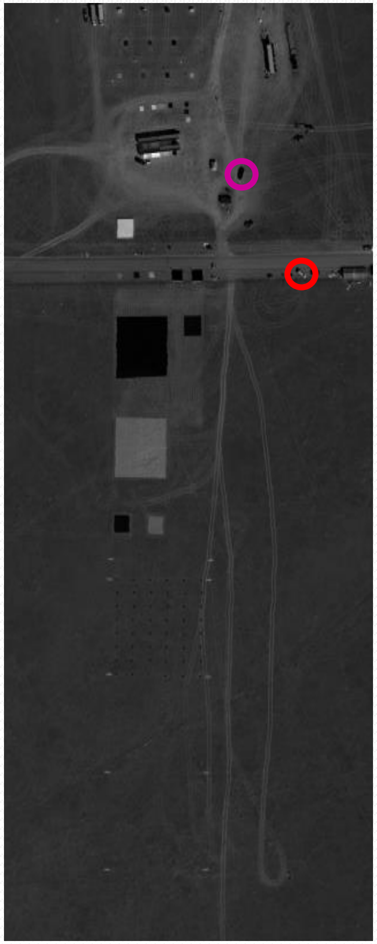

SN3515_20140812T173812_0002

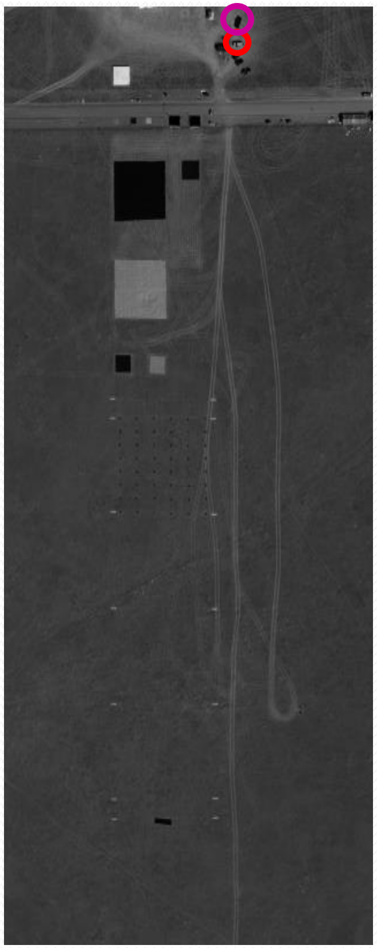

SN3515_20140812T171547_0002

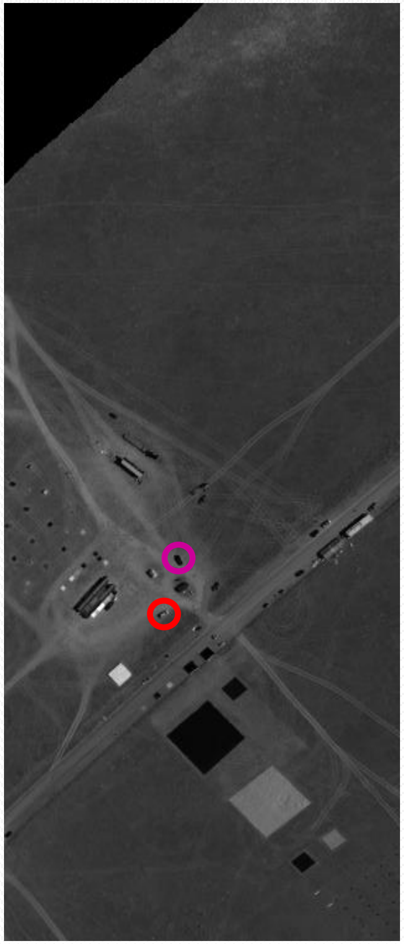

SN3515_20140812T172543_0002

Selected SWIR Images and Ground Truths Set 2 (NEO_Hyspex)

SWIR320meSN3515_20140820T145651_0002

SWIR320meSN3515_20140820T150923_0002

SWIR320meSN3515_20140820T150517_0003

Target Detection Results (Target 1/ Set1) Algorithm: SAM

Image No: 1

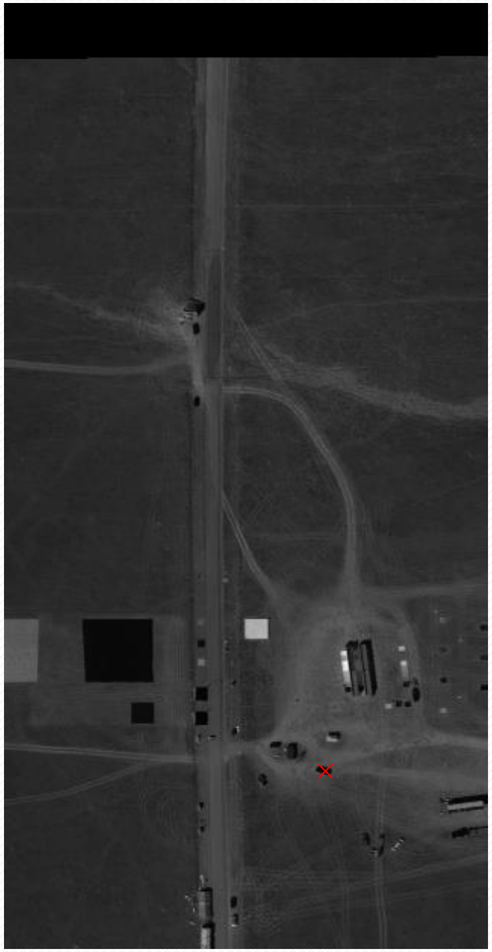

Image No: 2

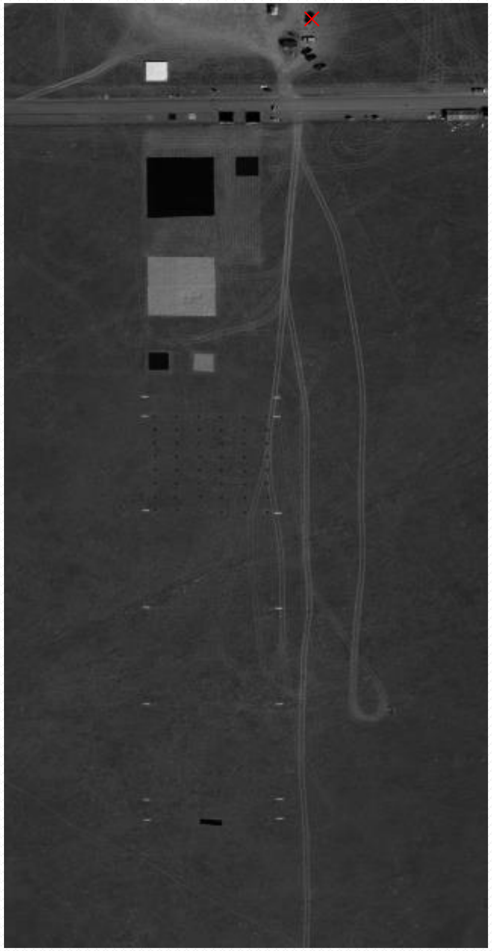

Image No : 3, Target with False Positives

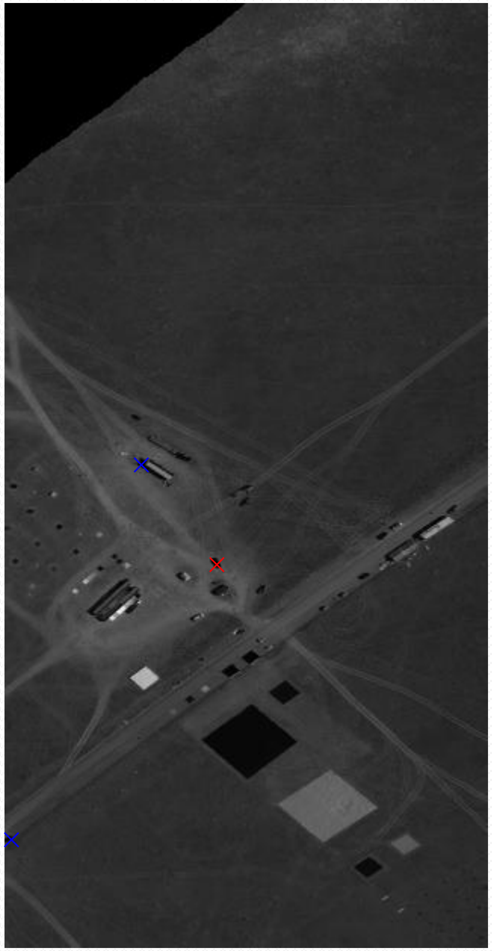

Target Detection Results (Target 1/ Set1) Algorithm: **SAM**

Image No: 4

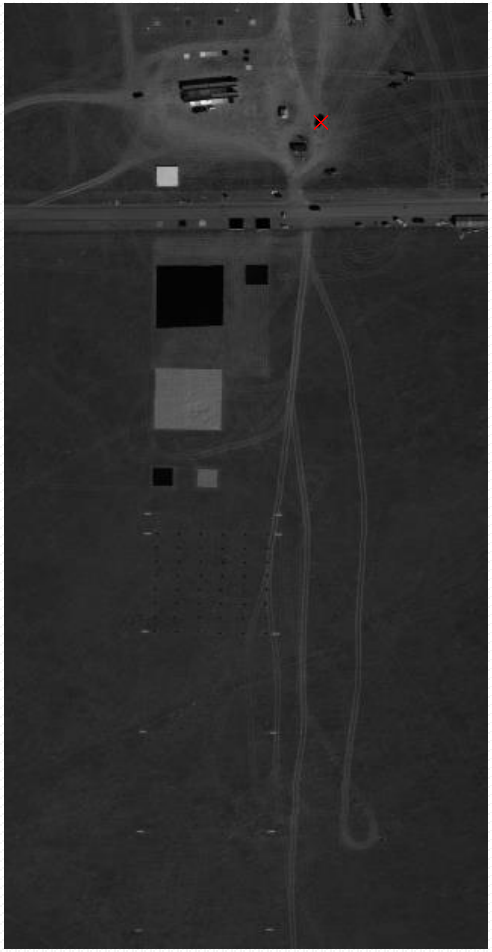

Image No: 5

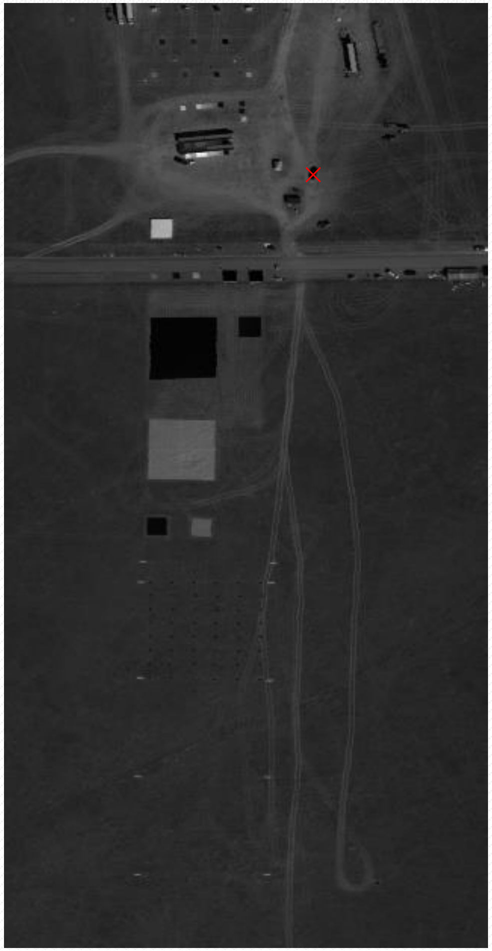

Target Detection Results (Target 1/ Set1) Algorithm: **ACE**

Image No: 1

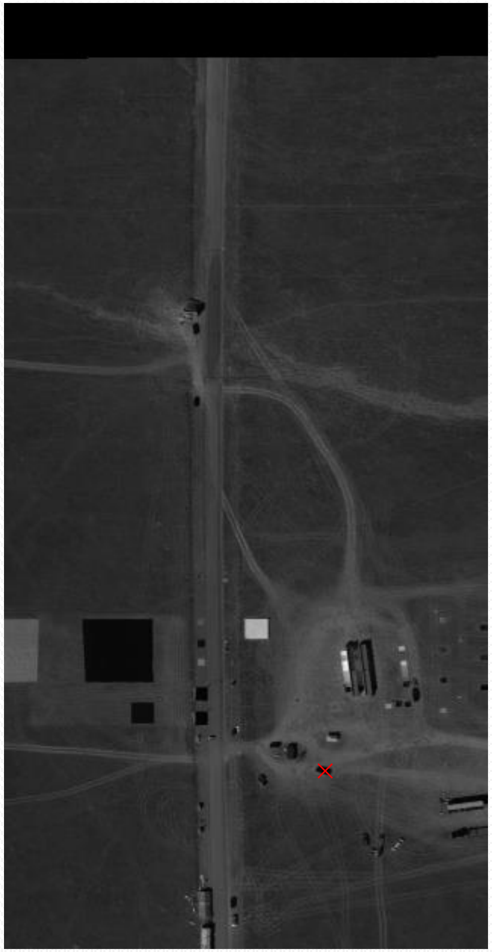

Image No: 2

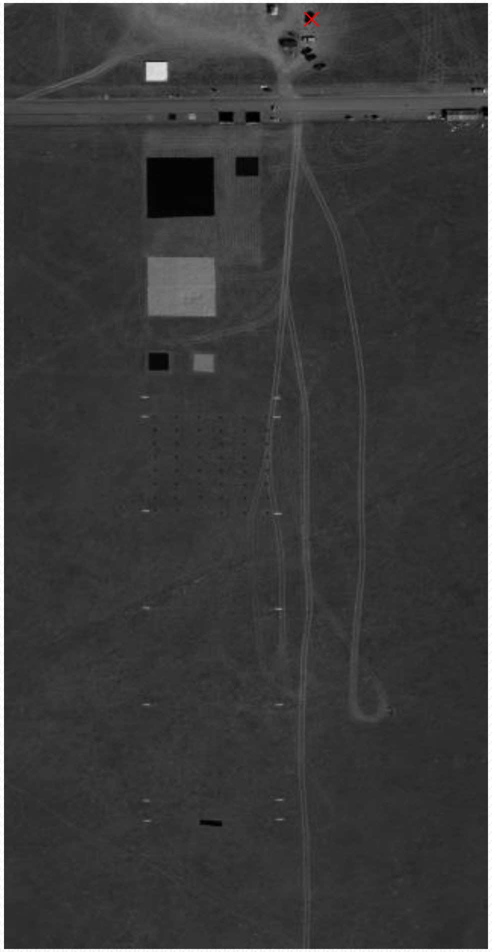

Image No : 3, Target with False Positives

Target Detection Results (Target 1/ Set1) Algorithm: **ACE**

Image No: 4

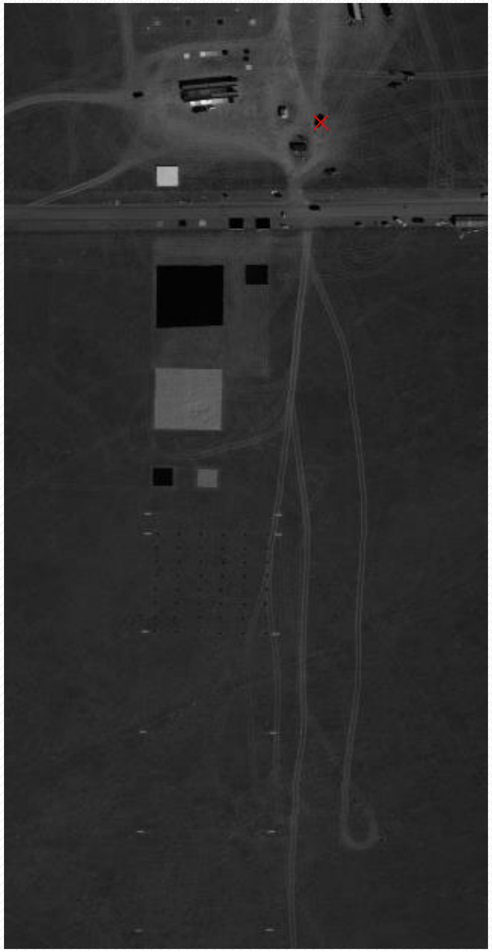

Image No: 5

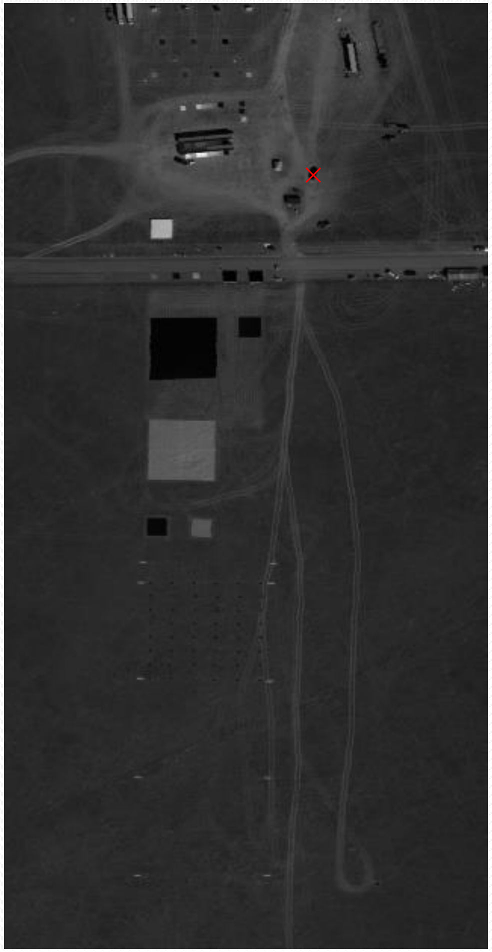

Target Detection Results (Target 1/ Set1) Algorithm: **OSP**

Background Signatures:

- One signature close to the target vehicle
- One signature far from the target
- One signature from the main road

Image No: 1

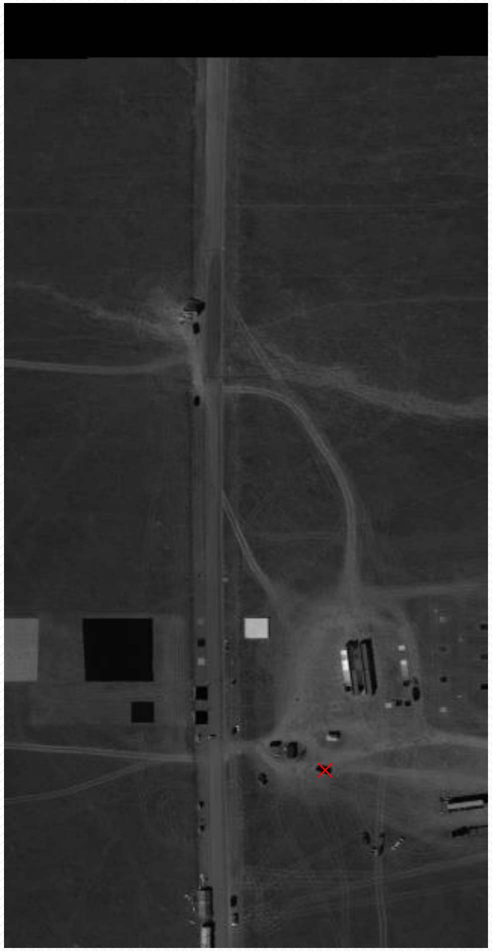

Image No: 2

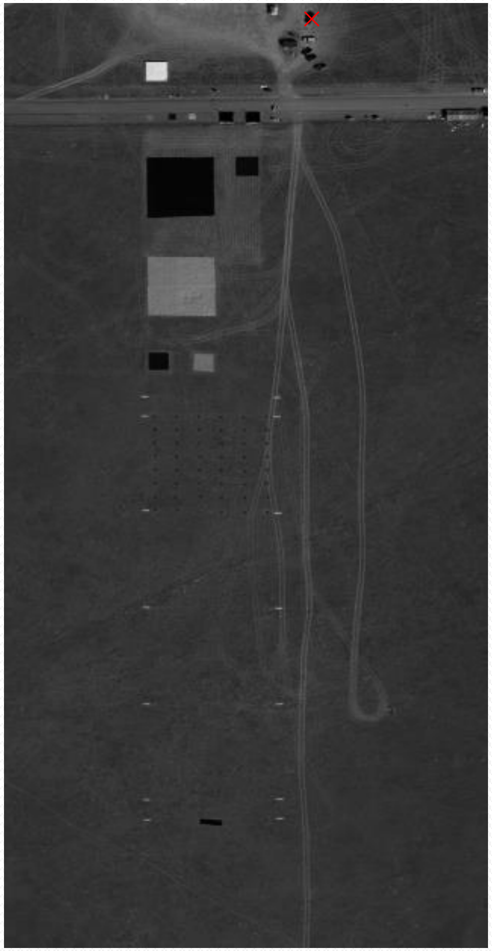

Target Detection Results (Target 1/ Set1) Algorithm: **OSP**

Image No : 3, Target with False Positives

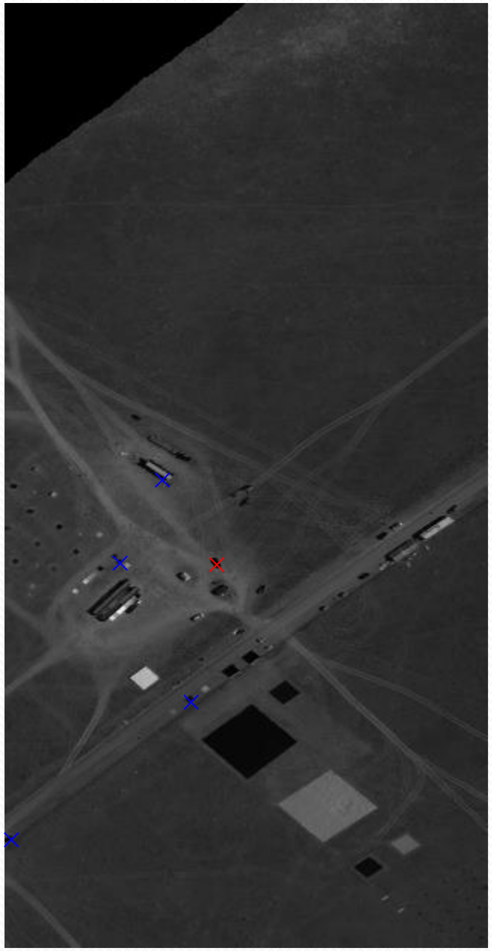

Image No : 4, Target with False Positives

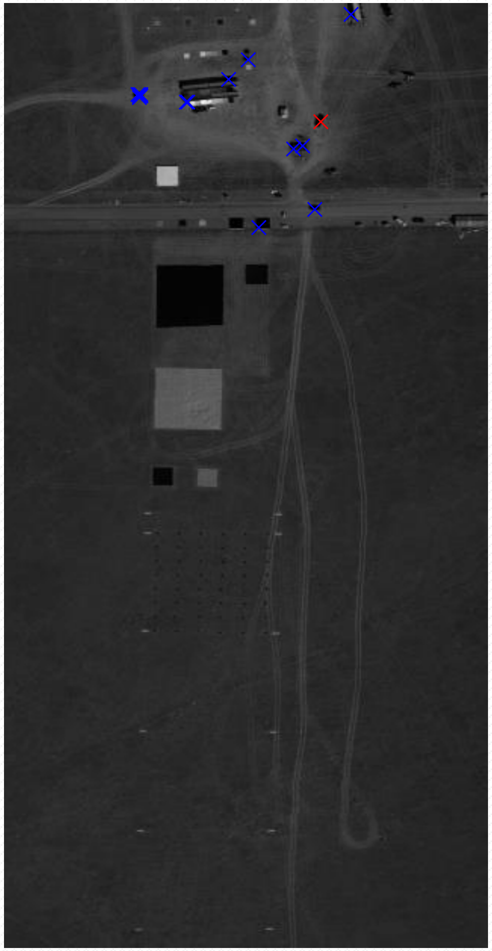

Image No : 5, Target with False Positives

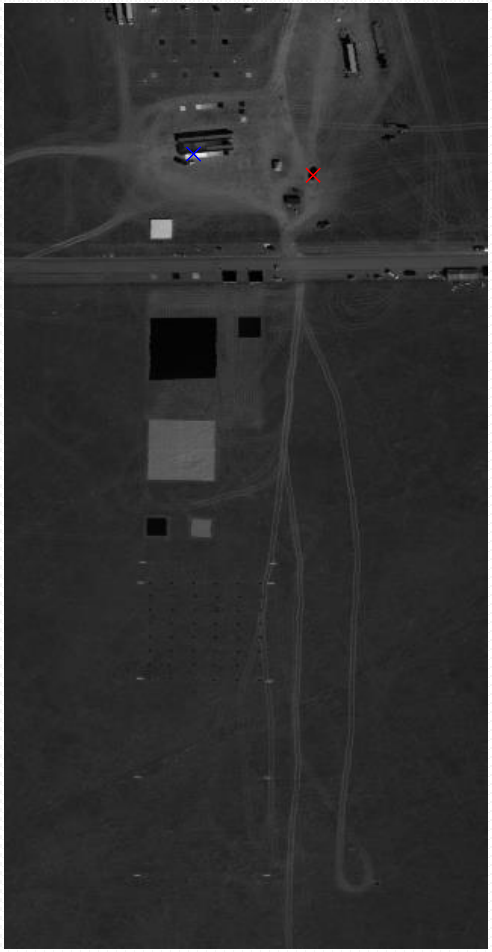

Target Detection Results (Target 1/ Set1) Algorithm: **HSD**

Background Signatures:
- One signature close to the target vehicle
- One signature far from the target
- One signature from the main road

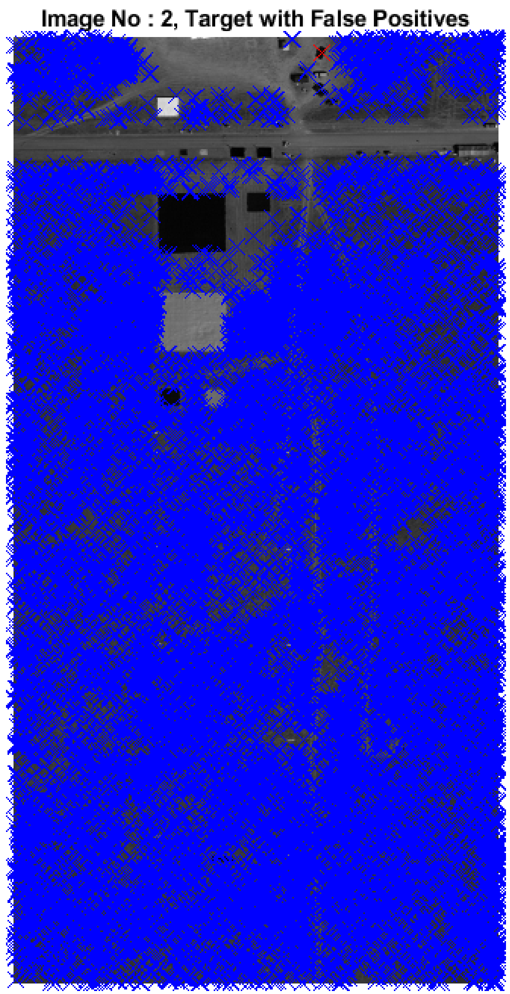

Selected LWIR Images and Ground Truths Set 1 (SEBASS)

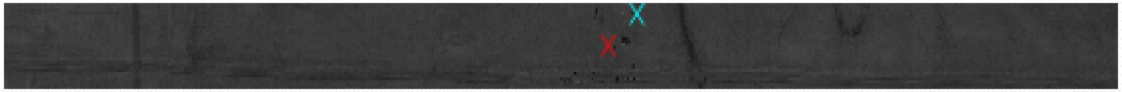

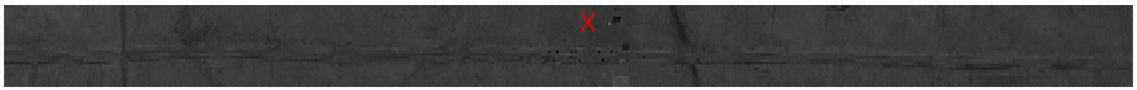

Set 1:

006_140811_181455_LINE_A30_l_L2S.dat

006_140811_184031_LINE_A30_l_L2S.dat

006_140811_183500_LINE_B30_l_L2S.dat

006_140811_181926_LINE_B30_l_L2S.dat

006_140811_182830_LINE_B30_l_L2S.dat

Selected LWIR Images and Ground Truths Set 2 (SEBASS)

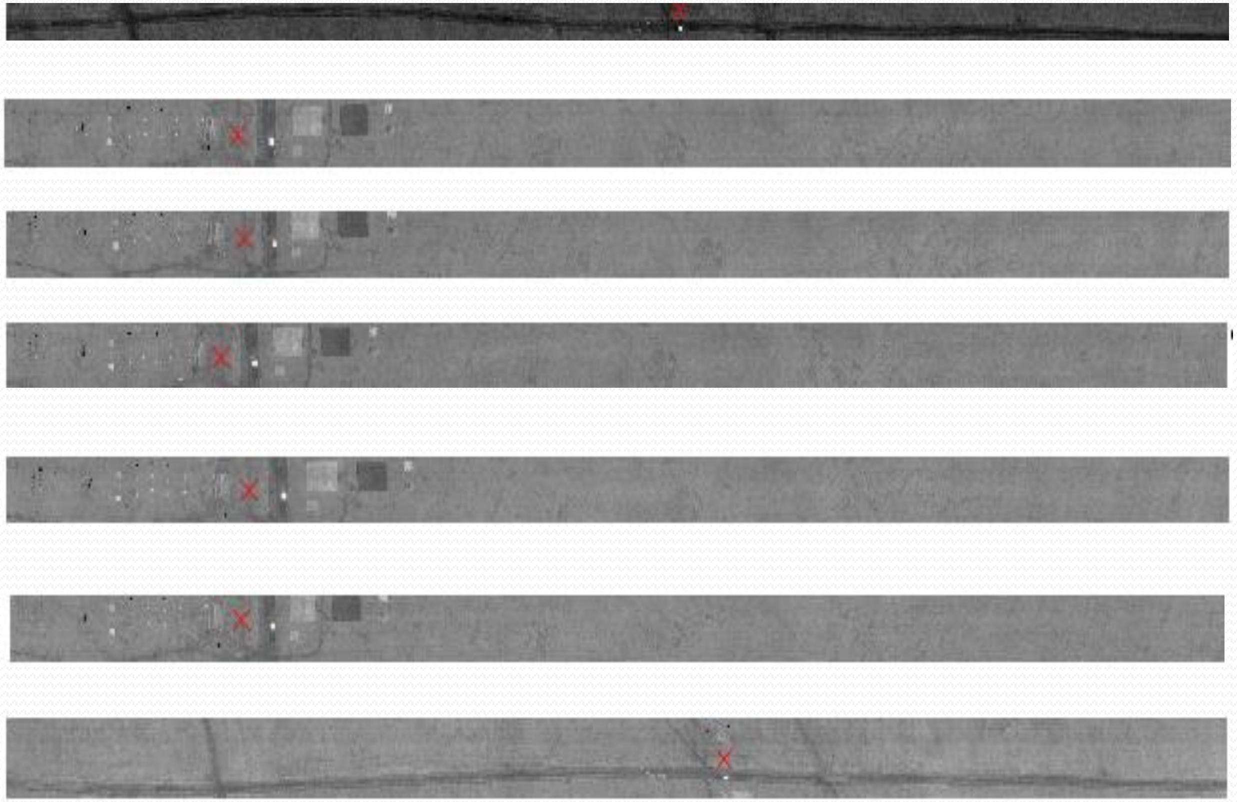

Set 2:

006_140824_214108_LINE_A15E_l_L2S.dat
006_140824_215013_LINE_B15N_l_L2S.dat
006_140824_215505_LINE_B15N_l_L2S.dat
006_140824_220015_LINE_B15N_l_L2S.dat
006_140824_220434_LINE_B15N_l_L2S.dat
006_140824_220908_LINE_B15N_l_L2S.dat
006_140824_221832_LINE_A30E_l_L2S.dat

Target Detection Results using **Radiance** Pixels vs. Group of Pixels (Algorithm ACE)

False Positive Counts

(Row: Reference radiance image no; Column: Test image no)

Image No		T1	T2	T3	T4	T5	Total	Rate (%)
R1	P	0	0	10	0	0	10	0.001
	SF	0	139	1	0	0	140	0.011
R2	P	6	0	1	0	0	7	0.001
	SF	3	0	0	0	0	3	0.001
R3	P	24	1	0	5	2	31	0.002
	SF	2	0	0	0	0	2	0.001
R4	P	41	20	0	0	2	63	0.005
	SF	28	0	0	0	0	28	0.002
R5	P	28	13	11	0	0	52	0.004
	SF	64	21	13	0	0	98	0.008

Target Detection Results using Radiance Pixels (Algorithm ACE)

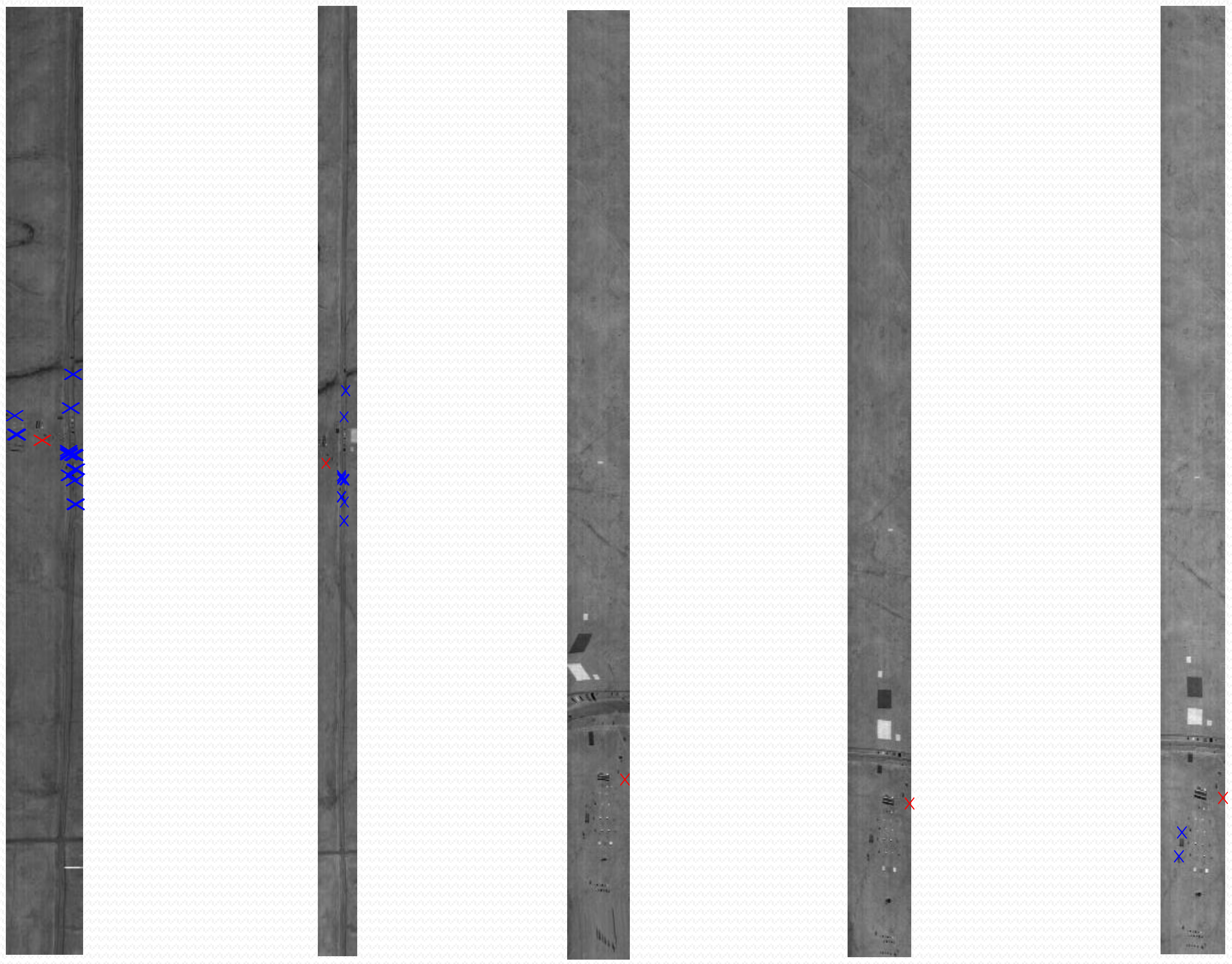

Target Detection Results using Radiance Group of Pixels (Algorithm ACE)

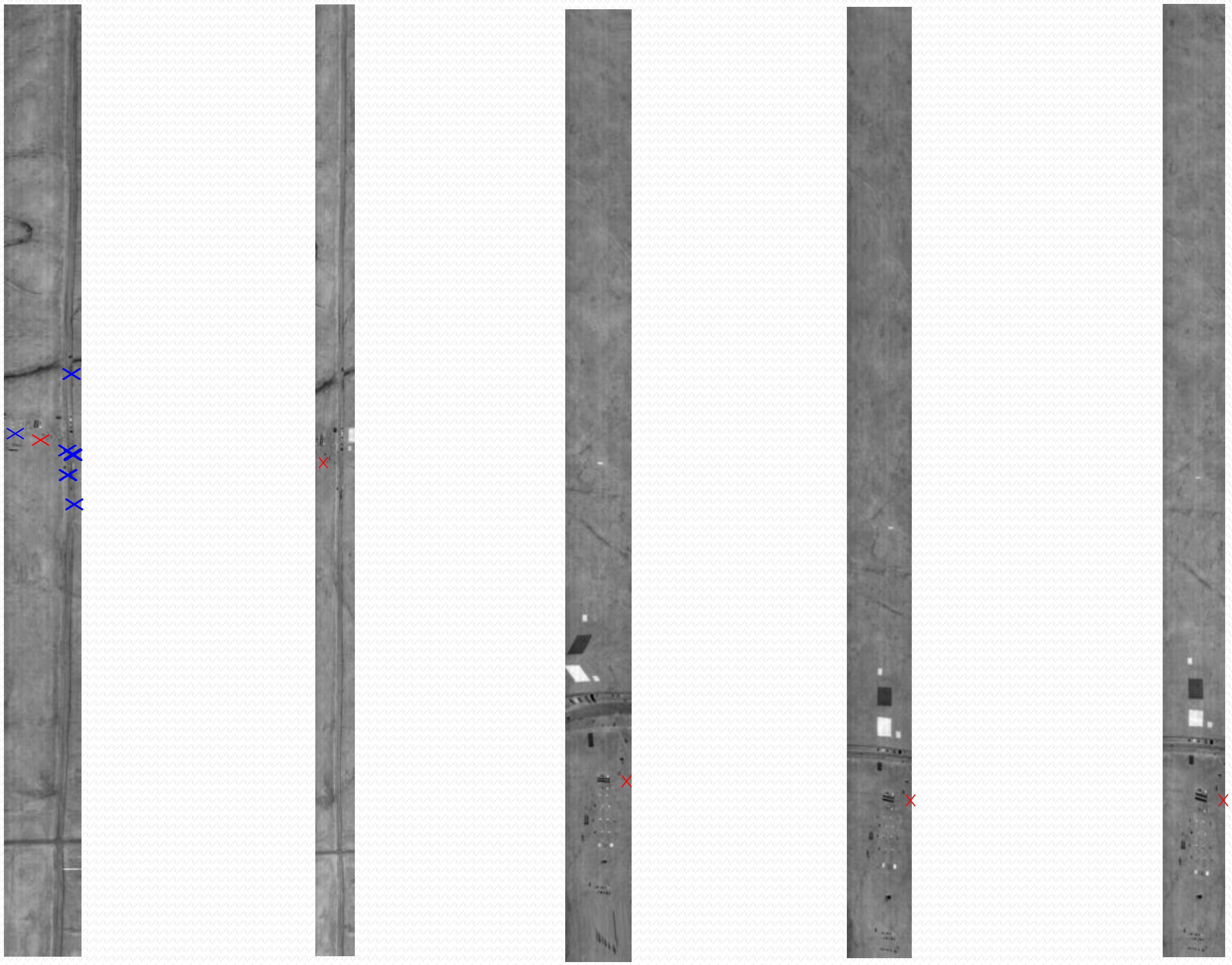

Target Detection Results using Radiance SUPERPIXELS (Algorithm ACE)

- Not Satisfactory Results with Superpixes
  - ➢ Superpixels are not very well aligned with the boundaries of the objects on thermal LWIR images

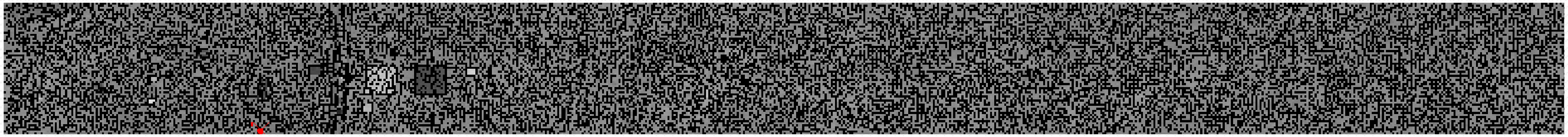

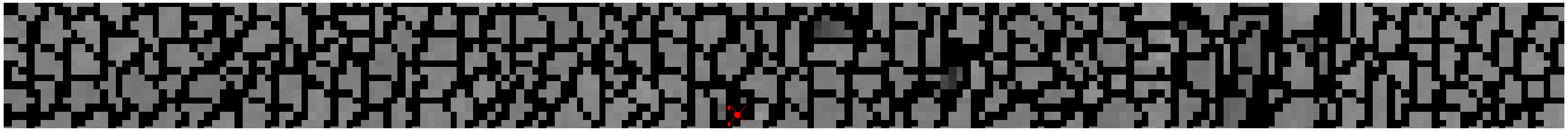

Target Detection Results using Emissivity Pixels (Algorithm ACE)

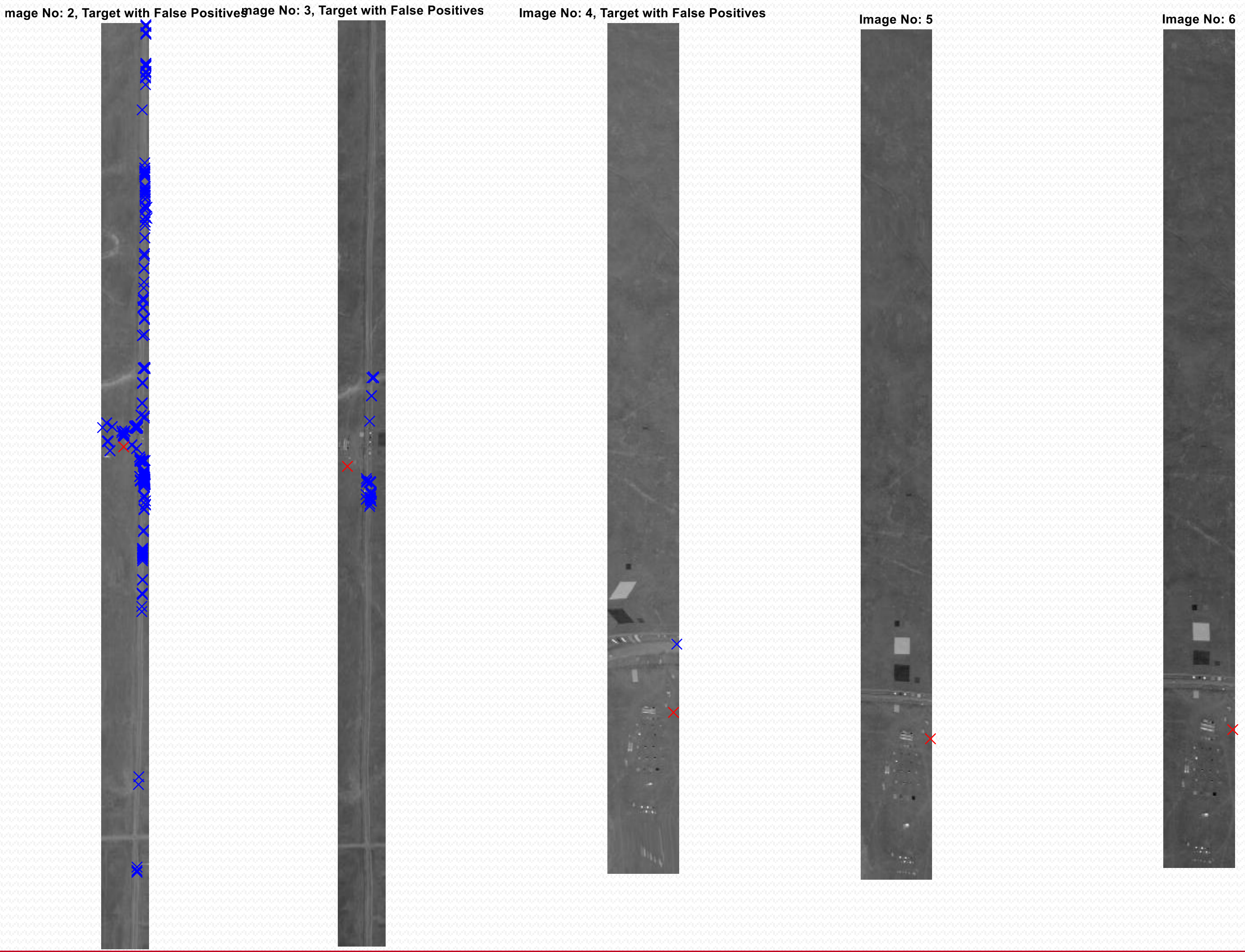

Target Detection Results using Emissivity Group of Pixels (Algorithm ACE)

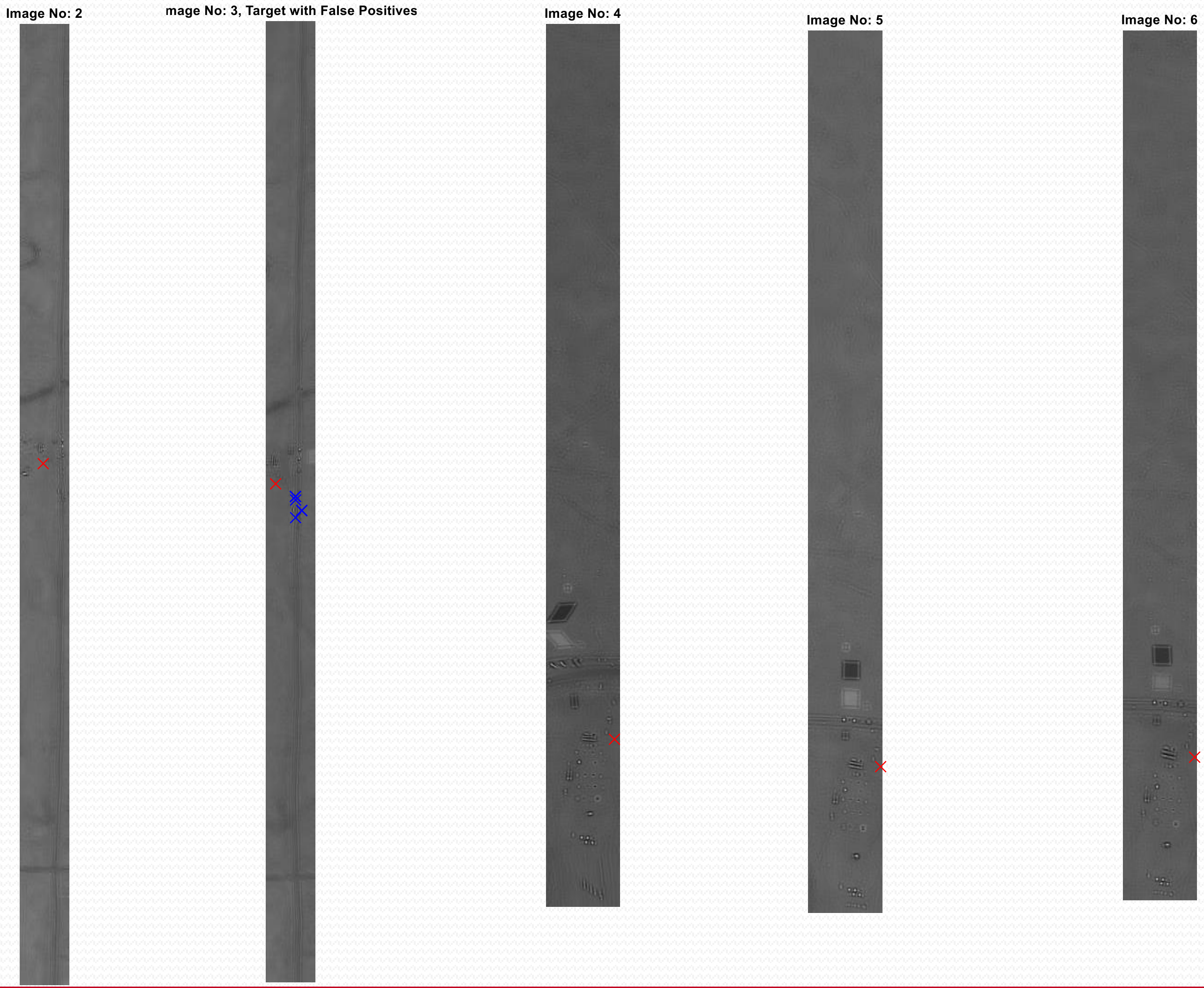

Target Detection Results over Radiance False Positive Rates

- Average False Positive Rates when True Positive Rate is 100%.
  - ACE is the leading algorithm.

	Matching Algorithm	Target 1 Set 1 (%)	Target 2 Set 1 (%)	Target 3 Set 1 (%)	Target 1 Set 2 (%)
Pixel Based	SAM	2.3652	0.0856	0.6310	0.0028
	ACE	0.0027	0.0009	0.0003	0.0013
	OSP	0.7340	0.0087	0.0003	0.0127
	HSD	1.3569	0.0004	0.0003	0.0001
Group of Pixels Based	SAM	12.0139	1.9467	0.1265	3.0756
	ACE	0.0044	0.0001	0.0002	0.0264
	OSP	6.1819	5.2492	0.0011	3.9974
	HSD	20.6007	8.9464	0.0010	0.0903

Target Detection Results over Radiance
Percentage of the Test Images with No False Positives

- Percentage of the test images where the target is detected without any false alarm.
  - ➢ ACE is the leading algorithm.

	Matching Algorithm	Target 1, Set 1 (%)	Target 2, Set 1 (%)	Target 3 Set 1 (%)	Target 1 Set 2 (%)
Pixel Based	SAM	5	25	17	59
	ACE	35	83	67	43
	OSP	30	42	67	45
	HSD	15	75	50	79
Group of Pixels Based	SAM	10	25	67	69
	ACE	60	83	50	59
	OSP	10	8	50	50
	HSD	20	75	67	69

Target Detection Results over Emissivity
Percentage of the Test Images with No False Positives

- Percentage of the test images where the target is detected without any false alarm.
  - ➢ ACE is the leading algorithm.

	Matching Algorithm	Target 1, Set 1 (%)	Target 2, Set 1 (%)	Target 3 Set 1 (%)	Target 1 Set 2 (%)
Pixel Based	SAM	17	17	55	5
	ACE	83	33	52	20
	OSP	58	33	57	30
	HSD	66	50	64	25
Group of Pixels Based	SAM	25	50	62	25
	ACE	75	83	67	60
	OSP	33	67	67	30
	HSD	37	67	69	20

Radiance vs. Emissivity
Percentage of the Test Images with No False Positives

- Percentage of the test images where the target is detected without any false alarm

Set ID	Target ID	Radiance	Emissivity
Set 1	Target 1 (black)	35 %	20 %
	Target 2 (white)	83 %	83 %
	Target 3 (black)	67 %	33 %
Set 2	Target 1 (black)	43 %	52 %

- ➢ Emissivity conversion does not affect the detection rate for the white car.
- ➢ Emissivity conversion does not indicate a <u>stable performance increase or decrease</u> for the black cars as well.

SWIR vs. LWIR

Percentage of the Test Images with No False Positives

- Percentage of the test images where the target is detected without any false alarm

	Target 1	Target 2	Target 3	Target 4
SWIR	75	85	83	100
LWIR	60	83	50	59

- ➢ Although the utilized targets are different in the experimental sets, the average detection rate in SWIR is better than the ones in LWIR.
- ➢ Better SNR quality in SWIR images compared to the ones in LWIR images, where the noise in thermal bands are more dominant.

Target Discovery Conclusions

The performances are compared with respect to the false positive rates when the recall (true positive rate) is 100 %. The percentage of the test images, where the target is detected without any false positives, over all the images, is employed as a second performance metric.

- **<u>Pixels vs. Group of Pixels vs Superpixels Comparison</u>**
  - GPs have indicated a significantly better result w.r.t Pixels.
  - Not Satisfactory Results with Superpixels as they are not very well aligned with the boundaries of the objects on thermal LWIR images
- **<u>Radiance vs. Emissivity Comparison</u>**
  - There is not a comparatively better result when emissivity is used in pixel wise detection. An exception is observed in the detection performances of white vehicle when the emissivity is utilized.
- **<u>Algorithm Comparison (SAM, ACE, OSP, HSD)</u>**
  - SAM and ACE have comparable performances for the SWIR Images.
  - ACE have indicated the best performance for LWIR images.
- **<u>SWIR vs LWIR Comparison</u>**
  - The detection performances for SWIR images are quite better compared to the LWIR images due to the better resolution and SNR for SWIR images.

REFERENCES

[1] J. Kerekes, M. Muldowney, K. Strackerjan, L. Smith, and B. Leahy. Vehicle tracking with multi-temporal hyperspectral imagery. In Defense and Security Symposium, pages 62330C–62330C. International Society for Optics and Photonics, 2006.

[2] B. Uzkent, A. Rangnekar, and M. Hoffman. Aerial vehicle tracking by adaptive fusion of hyperspectral likelihood maps. The IEEE Conference on Computer Vision and Pat- tern Recognition Workshops (CVPRW), July 2017.

[3] Blake M. Rankin, Joseph Meola, and Michael T. Eismann, "Spectral Radiance Modeling and Bayesian Model Averaging for Longwave Infrared Hyperspectral Imagery and Subpixel Target Identification" IEEE Trans. Geosci. Remote Sensing, vol. 55, no. 12, 2016.

[4] Nathan P. Wurst, Seung Hwan An, Joseph Meola, “Comparison of longwave infrared hyperspectral target detection methods”, Proc. SPIE 10986, Algorithms, Technologies, and Applications for Multispectral and Hyperspectral Imagery XXV, 1098617, May 2019.

Thanks.